

A Concatenated Residual Convolutional Network for Image Deblurring

Li Si-Yao¹, Dongwei Ren², Zijian Hu¹, Junfeng Li¹, Qian Yin^{1*}, Ping Guo^{1,3}

¹ Beijing Normal University ² Tianjin University ³ Beijing Institute of Technology

lisiyao@mail.bnu.edu.cn, {rendongwei, hanshz1998}@gmail.com,

{lijunfeng, yinqian}@bnu.edu.cn, pguo@ieee.org

Abstract

Deep convolutional neural network (CNN)-based restoration methods have recently received considerable progress in low level vision tasks, e.g., denoising, super-resolution, inpainting. A plain CNN, however, fails in image deblurring due to the severe pixel superposition caused by blur degradation. In this paper, we propose a novel concatenated residual CNN for image deblurring. Driven by minimum mean square error (MMSE)-based discriminative learning, the solution to image deblurring is interestingly unfolded into a series of iterative residual components, and is analyzed to demonstrate the contribution of iterative residual deconvolution (IRD). Furthermore, IRD motivates us to take one step forward to design CNN for image deblurring. Specifically, a residual CNN unit is employed to substitute the residual iteration, and is then concatenated and finally integrated, resulting in concatenated residual convolutional network (CRCNet). The experimental results demonstrate that CRCNet can not only achieve better quantitative metrics but also recover more visually plausible texture details.

1 Introduction

Image deblurring that aims at recovering a clear image from its blurry observation receives considerable research attention in decades. The blurry image b is usually modeled as a convolution of clear image x and blur kernel k , i.e.,

$$b = k * x + \eta, \quad (1)$$

where $*$ denotes 2D convolution, and η is additive noise. Thus, image deblurring is also well known as image deconvolution [Andrews and Hunt, 1977; Kundur and Hatzinakos, 1996]. When blur kernel k is given, clear images can be recovered by deconvolution under the maximum a posterior (MAP) framework [Andrews and Hunt, 1977; Fergus *et al.*, 2006; Levin *et al.*, 2007; Krishnan and Fergus, 2009],

$$\hat{x} = \arg \min_x \frac{1}{2} \|k * x - y\|^2 + \lambda \mathcal{R}(x), \quad (2)$$

where $\mathcal{R}(x)$ is regularization term associated with image prior, and λ is a positive trade-off parameter.

In conventional deconvolution methods, considerable research attention is paid on the study of regularization term for better describing natural image priors, including Total Variation (TV) [Ren *et al.*, 2015; Wang *et al.*, 2008], hyper-Laplacian [Krishnan and Fergus, 2009], dictionary sparsity [Zhang *et al.*, 2010; Hu *et al.*, 2010], non-local similarity [Dong *et al.*, 2013], patch-based low rank prior [Ren *et al.*, 2016]. Note that alternative direction method of multipliers (ADMM) is often employed to efficiently solve these models. Besides, driven by the success of discriminative learning, the image priors can be learned from abundant training samples. With the half-quadratic splitting strategy, regression tree field [Jancsary *et al.*, 2012; Schmidt *et al.*, 2013] and shrinkage field [Schmidt and Roth, 2014] are proposed to model regularization term, and are effectively trained stage-by-stage. These learning-based methods have validated the superiority of discriminative learning over manually selected regularization term [Schmidt *et al.*, 2013; Schmidt and Roth, 2014].

Most recently, deep convolutional neural network (CNN), as a general approximator, has been successfully applied in low level vision tasks, e.g., image denoising [Zhang *et al.*, 2017], inpainting [Yang *et al.*, 2017], superresolution [Dong *et al.*, 2014]. As for image deblurring, there are also several attempts, in which CNN is used to directly map blurry images to clear ones. In [Nah *et al.*, 2017], a deep multi-scale CNN is designed in image deblurring without explicit blur kernel estimation. In [Kupyn *et al.*, 2017], a generative adversarial network (GAN) tries to train a ResNet [He *et al.*, 2016] supervised by the adversarial discriminator. However, these trained CNN-based models can only handle mildly blurry images, and usually fail in real cases, since practical blur trajectories are complex.

When the blur kernel is known, CNN-based deconvolution has also been studied. On one hand, Xu *et al.* [2014a] have validated that plain CNN cannot succeed in deconvolution. To make CNN work well for deconvolution, a specific blur kernel would be decomposed into inverse kernels [Xu *et al.*, 2014b], which are then used to initialize CNN, inevitably limiting its practical applications. On the other hand, CNN is incorporated into conventional deconvolution algorithms under plug-and-play strategy. In [Chan *et al.*, 2016],

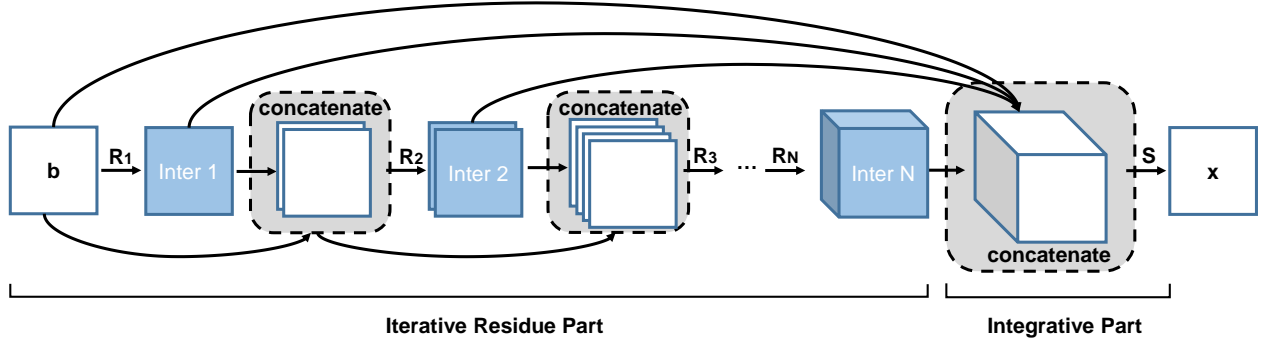


Figure 1: The architecture of CRCNet. In this demonstration, R_i is the i -th Residue Unit and S represents the Integrative Unit.

CNN is employed to solve denoising subproblem in ADMM modulars. In [Zhang *et al.*, 2017], CNN-based Gaussian denoisers are trained off-line, and are iteratively plugged under half-quadratic strategy. Although these methods empirically achieve satisfactory results, they are not trained end-to-end, and some parameters need to be tuned for balancing CNN strength. As a summary, the effective CNN architecture for deconvolution still remains unsolved.

In this paper, we propose a novel concatenated residual convolutional network (CRCNet) for deconvolution. Driven by the minimum mean square error (MMSE)-based discriminative learning, a closed-form deconvolution solution is derived. Interestingly, by a series expansion, this solution can be further unfolded into an iterative residual deconvolution (IRD) algorithm. IRD is a very simple yet effective deconvolution scheme. As shown in Figure 2, the blur can be effectively removed with the increasing of iterations. But IRD is sensitive to noise, and would magnify the noise, as shown in Figure 2. Motivated by this observation, we design an effective CNN architecture for deconvolution, as shown in Figure 1. We adopt residual CNN unit to substitute the residual component in IRD. These residual CNN units are iteratively concatenated, and are finally integrated, resulting in CRCNet. The contribution of CRCNet architecture is experimentally analyzed. We claim that effective CNN architecture plays the critical role in deconvolution, and CRCNet is one of the successful attempts. Moreover, on a test dataset, CRCNet can achieve higher quantitative metrics and recover more visually plausible texture details, compared with state-of-the-art algorithms.

Our contributions are three-fold:

- We derive a closed-form deconvolution solution driven by MMSE-based discriminative learning, and further unfold it as a simple yet effective IRD algorithm.
- Motivated by IRD algorithm, we propose a novel CRCNet for deconvolution. The CRCNet can be trained end-to-end, but is not a plain CNN architecture and is well analyzed.
- We discuss the contributions of CRCNet, and show the critical role of network architecture for deconvolution. Experimental results demonstrate the superiority of CRCNet over state-of-the-art algorithms.

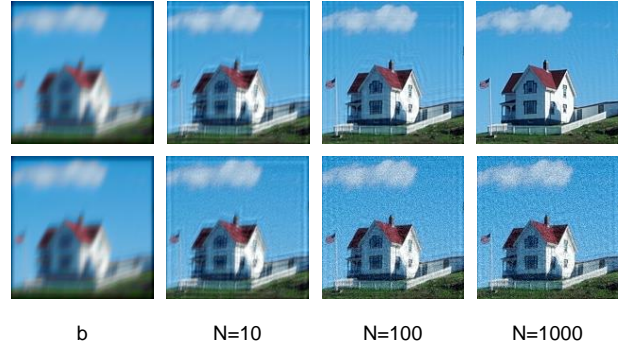


Figure 2: Deblurring results using $H^T \sum_{n=0}^N (\sigma' I - H H^T)^n$ with different N . The first row: deblurring image without noise; the second row: deblurring noisy image with $\sigma = 0.01$. Here pixels of natural images are assumed to be independent and $C_x = I$. For visualization, the deblurring is operated on the first channel of YCbCr.

The reminder of this paper is organized as follows: Section 2 derives MMSE-based deconvolution, and then presents IRD algorithm. Section 3 designs CRCNet based on IRD, along with its training strategy. Section 4 demonstrates experimental results and Section 5 ends this paper with conclusions.

2 Iterative Residue Deconvolution

In this section, we first derive a deconvolution solution driven by minimum mean square error (MMSE) [Andrews and Hunt, 1977], which is then unfolded via series expansion, resulting in iterative residual deconvolution (IRD) algorithm. Finally we give an insightful analysis to IRD, and provide a potential CNN architecture for deconvolution.

2.1 MMSE Deconvolution

The convolution operation in Eqn. (1) can be equivalently reformatted as a linear transform

$$\underline{k} * \underline{x} = H \underline{x}, \quad (3)$$

where H is a Blocked Toeplitz Matrix [Andrews and Hunt, 1977; Gray, 2006] and \underline{A} represents the column-wise expansion vector of matrix A . Then we aim to seek a linear transform L to recover clear image

$$\hat{\underline{x}} = L \underline{b}. \quad (4)$$

Let us assume a set of training image pairs $\{x, b\}$. By minimizing MSE loss, we have

$$\begin{aligned} L &= \arg \min_L \mathbb{E}_x [\text{Tr}(\underline{x} - \hat{x})(\underline{x} - \hat{x})^T] \\ &= C_x H^T (H C_x H^T + C_\eta)^{-1}, \end{aligned} \quad (5)$$

where $C_x = \underline{x}\underline{x}^T$ and $C_\eta = \underline{\eta}\underline{\eta}^T$ are Gramm matrices of clear images and noises, respectively. $C_x[i, j]$ represents the correlation between the i -th pixel and the j -th pixel of a sharp image and C_η is similar.

On one hand, correlations among pixels of natural images are limited [Hu *et al.*, 2012], thus eigenvalues of C_x can be deemed to be positive. Then, for any possible C_x , we can always find an $\alpha > 0$ such that $\lambda_{max}(\alpha C_x) \leq 1$ where λ_{max} represents the greatest eigenvalue. Hence, we have

$$\begin{aligned} L &= C_x H^T ((1/\alpha)(H \alpha C_x H^T + \alpha C_\eta))^{-1} \\ &= C'_x H^T (H C'_x H^T + C'_\eta)^{-1}, \end{aligned} \quad (6)$$

where $C'_x = \alpha C_x$ and $C'_\eta = \alpha C_\eta$.

On the other hand, η is deemed to be zero-meaned gaussian noise with strength σ/α (assumed small in this work), thus C'_η approximates to σI . Hence, L can be approximated as

$$L \approx C'_x H^T (H C'_x H^T + \sigma I)^{-1}. \quad (7)$$

To now, we have obtained a closed-form solution for deconvolution.

2.2 IRD Algorithm

For matrix A with $A^n \rightarrow 0$ as $n \rightarrow \infty$, the series expansion holds

$$(I - A)^{-1} = \sum_{n=0}^{\infty} A^n. \quad (8)$$

As for the case in deconvolution, blur kernel k is under two constraints [Kundur and Hatzinakos, 1996; Levin *et al.*, 2009; Perrone and Favaro, 2014]:

$$k_{ij} \geq 0 \quad (9)$$

and

$$\sum_{i,j} k_{ij} = 1. \quad (10)$$

Under such constraints, the norm of degradation matrix H is limited under 1. We also found empirically that eigenvalues of $H H^T$ are generally positive.

Thus, the linear deconvolution solution L in Eqn. (7) can be unfolded as follows:

$$L \approx [C'_x H^T] \left[\sum_{n=0}^N (\sigma' I - H C'_x H^T)^n \right] \quad (11)$$

where $\sigma' = 1 - \sigma$. Eqn. (11) can be implemented as an iterative algorithm. Matrix multiplications by H and H^T are equal to convolutions with k and the flipped kernel k_- .¹ The correlation matrix C'_x actually plays as the prior of clear images and is assured to be Toeplitz [Andrews

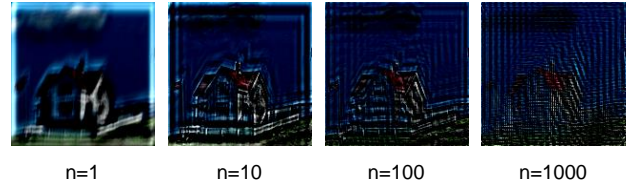


Figure 3: Intermediate components $H^T(\sigma' I - H H^T)^n b$ corresponding to the first row in Figure 2 with increasing n . The operation is taken on the first channel of YCbCr. The original pixel values are too small when n is large, thus images are scaled by $1.5, 10^2, 10^3, 2 \times 10^4$ respectively to keep the maximum equal to 1 for visualization.

and Hunt, 1977]. Hence, linear transform C'_x is equivalent to a convolution with a limited patch f_x for pixels of clear images are correlated only in the vicinity. By assuming pixels in a clear image are independent [Hu *et al.*, 2012; Ren *et al.*, 2018], C'_x can be simplified as identity matrix I , i.e., $f_x = \delta$. The detailed process is summarized as IRD Algorithm 1.

Algorithm 1 Iterative Residue Deconvolution

Input: blurry image b , degradation kernel k , image priori patch f_x , noise strength σ

Output: restored \hat{x}

- 1: $\sigma' \leftarrow 1 - \sigma, s \leftarrow b, r \leftarrow b$
 - 2: **for** $i \leftarrow 0$ to $N - 1$ **do**
 - 3: $r \leftarrow \sigma' r - k * f_x * k_- * r$
 - 4: $s \leftarrow s + r$
 - 5: **end for**
 - 6: $\hat{x} \leftarrow f_x * k_- * s$
-

The IRD algorithm is very simple yet effective for deconvolution. Figure 2 shows that the clear image can be satisfactorily restored from a noise-free blurry one after 1000 iterations. Although the noise is significantly magnified for a noisy blurry image, the blur can also be effectively removed.

To explore the significance of unfolded components, we extracted $C'_x H^T (\sigma' I - H C'_x H^T)^n$ as shown in Figure 3. The energy of iterative residues attenuates but the component represents more detailed signals in higher frequency with increasing n . Each iteration extracts residual information from the result of the previous iteration, and those components are finally summed to a clear image.

Although the assumption $C_x = I$ does not hold for real cases, IRD can still remove blur effectively. More interesting, IRD provides a potential network structure for deconvolution. Representing MMSE deconvolution as a sum of power series reformulates the inverse process into residual convolutions, which reminds us the residual learning structure proposed by He *et al.* [2016]. All convolutional parts in IRD can be learned as weights of a CNN. Such an analogy inspired us to propose the following network structure.

¹The flip operation corresponds to $\text{rot90}(\cdot, 2)$ in MatLab.

3 Concatenated Residue Convolutional Network

By imitating IRD algorithm, we designed a network as shown in Figure 1, which includes two parts: the Iterative Residual Part and the Integrative Part, corresponding to $[(\sigma' I - HC'_x H^T)^n]$ and $[C'_x H^T \sum_{n=0}^N]$, respectively. For the first part, $\sigma' I - HC'_x H^T$ corresponds to the *conv-deconv-minus* structure of a Residual Unit. Consider that linear operator C_x is symmetric $C_x = C_x^{\frac{1}{2}} C_x^{\frac{1}{2}T}$, thus $HC_x H^T$ can be separated into $(HC_x^{\frac{1}{2}})(C_x^{\frac{1}{2}T} H^T)$. Note that operator H and C_x equal to convolutions (see section 2), so their transposes correspond to transpose convolutions (also called *deconvolutions* in CNN). For the second, operator $[C'_x H^T \sum_{n=0}^N]$ is implemented as *conv* layers on the concatenation of all residues with gradually decreased channels. Because a CNN manipulates convolutions channel-wisely and sum the convolutions of all channels, this structure can sum all residues while adopting convolutions.

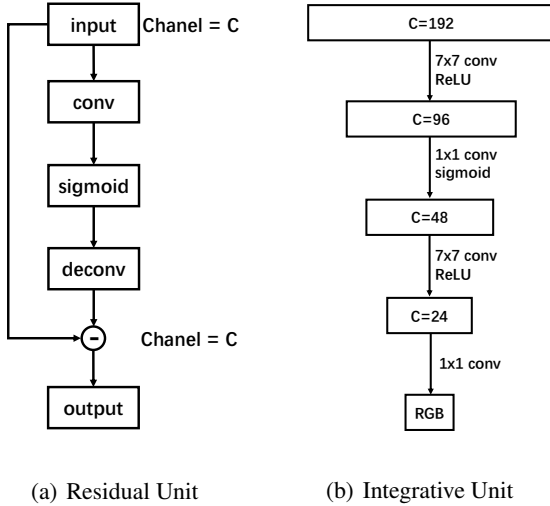


Figure 4: Demonstration of RU and IU.

Residue Unit. A Residue Unit (RU) calculates the difference between the input and the processed image to extract valid information. Figure 4 (a) shows the structure of an RU. The number of channels of processed image is kept the same as the input.

Compared to the Eqn. (11), in each RU, convolutional and deconvolutional (transpose convolutional) layers resemble $HC'_x H^T$. However, the auto-encoder-like network can realize more complicated transforms by taking advantage of non-linearity layers. Further, the weights of convolutional layers are learned from not only the blur but also clear images. Hence, an RU can extract information of images more efficiently.

In our experiments, kernel sizes of each *conv* and *deconv*

are 3×3 . We discovered that taking *sigmoid* function is more efficient than the rectified linear unit (ReLU) in RUs.

Iterative Concatenation. Our network concatenates outputs of previous units as the input of the next RU. As shown in Figure 1, R_i represents the i -th Residue Unit introduced before, $inter_i$ is the output of R_i , and the input of R_i is the concatenation of all previous outputs of R_j ($j < i$) along channels. Formally,

$$\begin{aligned} inter_i &= R_i(input_i), \\ input_i &= [inter_0, \dots, inter_{i-1}], \end{aligned} \quad (12)$$

where $inter_0$ and $input_0$ are the blurry input b .

The destination of concatenating previous outputs is to enhance the capability to extract details in deeper layers. Firstly, concatenations expand channels for convolutions of tensors and hence make sufficient transforms on deep residual information. Secondly, compared to trivial MMSE expansion Eqn. (11) where the i -th iteration is only applied on the $(i-1)$ -th result, concatenation $[inter_0, \dots, inter_{i-1}]$ makes the model more flexible.

In our experiment, inputs b are 256×256 RGB images. We took $N = 6$ and the dimension of the final concatenation before integration is 192.

Integration. The last part of our network is to integrate all extracted information from the blurry image. The input b and all intermediate residues are concatenated and fed into an Integrative Unit (IU). IU takes two 7×7 *conv* layers to play a role as $[C'_x H^T]$ and the channel dimension C decreases gradually to 3 through convolutions as a weighted sum of unfolded components. The detailed structure is shown in Figure 4 (b).

Loss Function. An ideal deblurring model is expected to restore sufficient content of clear image x and make the restored \hat{x} looks sharp. Thus, the loss function of our network is designed to consist of a *content loss* and an *edge loss*:

$$\mathcal{L} = \alpha \mathcal{L}_c + \gamma \mathcal{L}_e \quad (13)$$

where \mathcal{L}_c is the smooth L_1 loss [Girshick, 2015]:

$$\mathcal{L}_c(\hat{x}, x) = \text{smooth}_{L_1}(\hat{x} - x), \quad (14)$$

which is more robust on outliers than MSE loss, and

$$\mathcal{L}_e(\hat{x}, x) = \|\partial_h \hat{x} - \partial_h x\|^2 + \|\partial_v \hat{x} - \partial_v x\|^2, \quad (15)$$

in which ∂_h and ∂_v represent horizontal and vertical differential operator.

The *edge loss* constrains edges of \hat{x} to be close to those of x . Our experiment showed that adding \mathcal{L}_e could speed up the convergence of the network efficiently and make restored edges sharp.

4 Experimental Results

4.1 Training CRCNet

Training Dataset Preparation

Clear Image Set. Clear images are essential to train network weights. The dataset is expected to only consist of uniformly sharp and noise-free images with ample textures. We manually selected and clipped 860 256×256 RGB images from BSD500 [Martin *et al.*, 2001] and COCO [Lin *et al.*, 2014] dataset, during which we omitted all pictures with Bokeh Effect or motion blur.



Figure 5: Randomly generated 10 degradation kernels.

Degradation Kernels. We randomly generated 10 21×21 degradation kernels by using code from [Chakrabarti, 2016] for training and testing. The generated kernels are shown in Figure 5.

Training details

We used Adam [Kingma and Ba, 2014] optimizer with a mini-batch of size 1 for training. The initial learning rate is 10^{-3} and decay 0.8 per 1000 iterations. The network was only trained 16K iterations for each blur kernel to keep this process portable. In our experiment $\alpha = 5000$ and $\gamma = 100$. 10 clear images with ample details were selected for tests and the rest 850 were used for training. The CRCNet was implemented in Python with PyTorch and tested on a computer with GeForce GTX 1080 Ti GPU and Intel Core i7-6700K CPU.

4.2 Comparison with Competing Algorithms

Several test results are shown in Figure 7. Compared with state-of-art approaches including traditional MAP method us-

Levin <i>et al.</i>	Krishnan & Fergus	Zhang <i>et al.</i>	CRCNet
0.8529	0.7342	0.8405	0.8758
0.8226	0.7606	0.8213	0.8924
0.8519	0.8578	0.8623	0.8751
0.8341	0.8177	0.8441	0.9073
0.8420	0.7392	0.8403	0.8447
0.8540	0.8667	0.8798	0.9018
0.8726	0.7114	0.8662	0.8878
0.8475	0.7338	0.8522	0.8630
0.8275	0.7335	0.8244	0.8655
0.8428	0.8548	0.8549	0.8832
0.8448	0.7810	0.8486	0.8797

Table 1: SSIM on 10 kernels. The last row is the average. It should be noted here that SSIM only measures one-channel images, thus results here are on the first channel of YCbCr.

ing sparse [Levin *et al.*, 2007] and Hyper-Laplacian [Krishnan and Fergus, 2009] priors, and CNN-based method [Zhang *et al.*, 2017], CRCNet recovers more details in restored images, e.g., fur of Teddy bears and bright spray. Thus deblurred results of our method look more natural and vivid. The whole test results will be published as a supplementary file.

Quantitative evaluations of the average SSIM [Wang *et al.*, 2004] of 10 test images with 10 kernels are shown in Table 1. Our approach achieves higher performance both visually and quantitatively.

The implementation of this work and the clear image set will be published online at once after this paper is accepted. (For avoiding anonymous conflicts.)

4.3 Analysis to CRCNet

A question beyond the superior performance is whether the effectiveness of CRCNet depends on our proposed concatenated residual (CR) architecture or just a trivial ‘universal approximator’ relying on neural networks. To verify the contribution of CR structure, we give analysis to the intermediate results of CRCNet and its relationship to IRD algorithm.

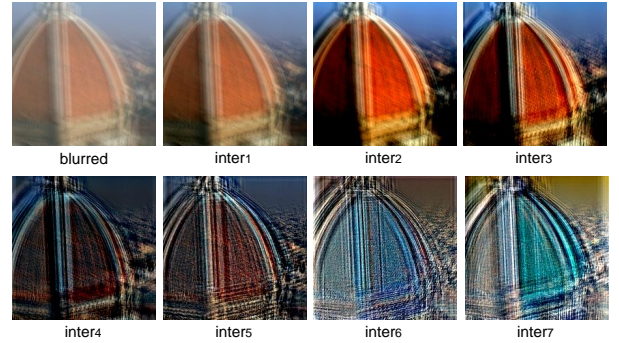


Figure 6: Intermediate outputs of CRCNet.

We visualized intermediate outputs of RUs ($inter_i$). It should be noted here that for visualization, we trained one more CRCNet with one-dimension (gray-scale) input and output and fed each channel of a blurry RGB image into this network and fold the outputs at the end. One channel of the each intermediate output are extracted. Figure 6 shows that higher frequency information are extracted from deeper layers, which actually resembles IRD algorithm, as shown in Figure 3. In IRD algorithm, a large number of iterations are required for satisfactory deblurring quality. But in CRCNet, due to the powerful modeling capability of CNN, a very small number of layers can provide good restoration quality. We in this paper claim that deep CNN-based model for deconvolution should be equipped with specific architecture instead of plain CNN, and our proposed CRCNet is one of the potential effective architectures.

5 Conclusions

In this paper, we proposed an effective deep architecture for deconvolution. By deriving the MMSE-based deconvolution solution, we first proposed an iterative residual deconvolution

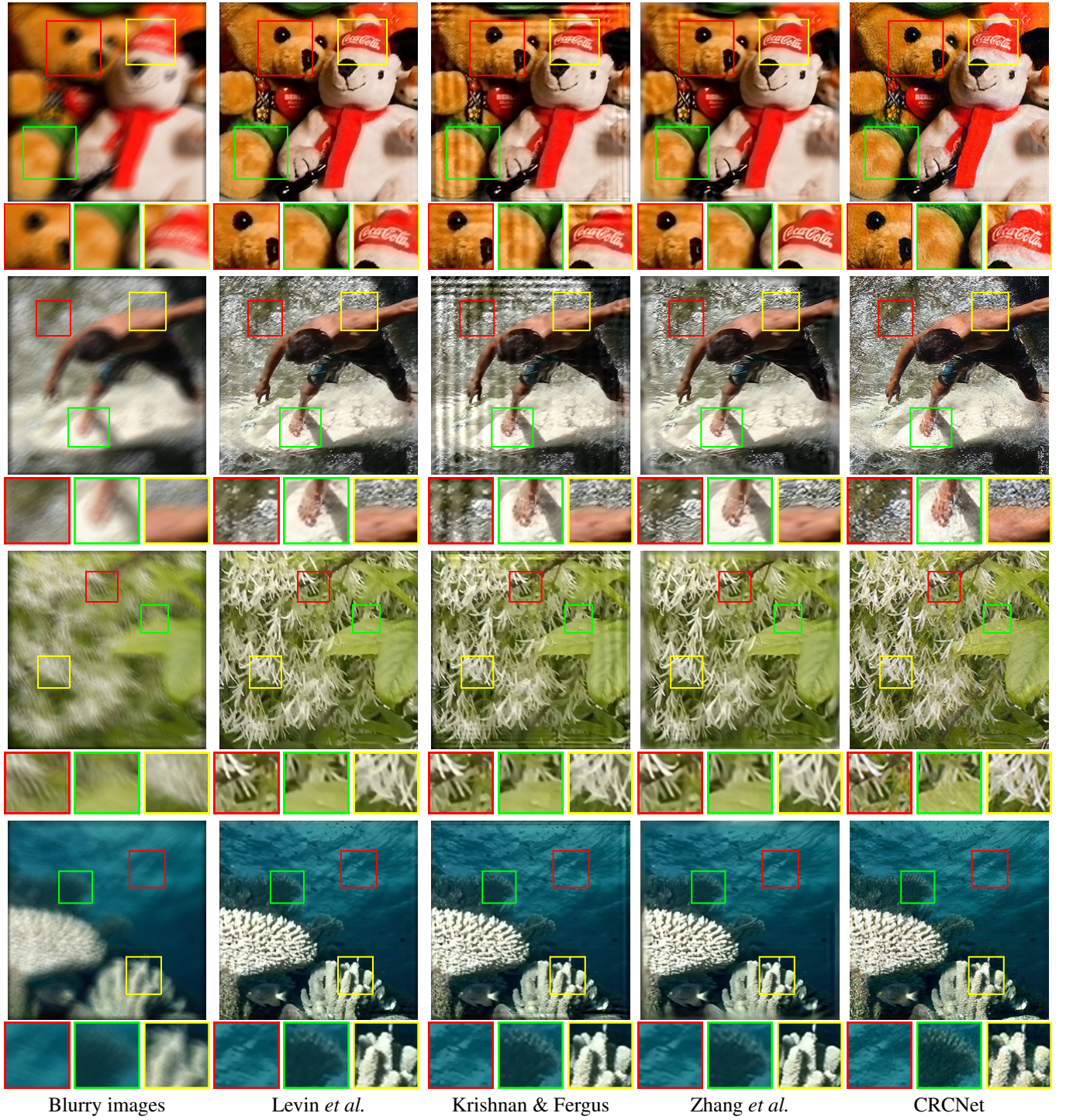


Figure 7: Visually comparison of deblurring results with state-of-art approaches.

algorithm, which is simple yet effective. We further designed a concatenated residual convolutional network with the basic architecture of IRD algorithm. The restored results by CRCNet are more visually plausible compared with competing algorithms. The success of CRCNet shows that deep CNN-based restoration architecture should borrow ideas from con-

ventional methods. In the future, we will develop more effective deep CNN-based restoration methods for other low level vision tasks.

References

- [Andrews and Hunt, 1977] Harry C. Andrews and Bobby Ray Hunt. *Digital image restoration*, chapter 7.2, pages 132–140. Prentice-Hall, Englewood Cliffs, NJ, 1977.
- [Chakrabarti, 2016] Ayan Chakrabarti. A neural approach to blind motion deblurring. In *ECCV*, pages 221–235. Springer, 2016.
- [Chan et al., 2016] Stanley H. Chan, Xiran Wang, and Omar A. Elgendy. Plug-and-play admm for image restoration: Fixed-point convergence and applications. *IEEE Transactions on Computational Imaging*, 3:84 – 98, 2016.
- [Dong et al., 2013] Weisheng Dong, Guangming Shi, and Xin Li. Nonlocal image restoration with bilateral variance estimation: a low-rank approach. *IEEE Transactions on Image Processing*, 22(2):700–711, 2013.
- [Dong et al., 2014] Chao Dong, Chen Change Loy, Kaiming He, and Xiaoou Tang. Learning a deep convolutional network for image super-resolution. In *ECCV*, pages 184–199. Springer, 2014.
- [Fergus et al., 2006] Rob Fergus, Barun Singh, Aaron Hertzmann, Sam T Roweis, and William T Freeman. Removing camera shake from a single photograph. In *ACM Transactions on Graphics*, volume 25, pages 787–794. ACM, 2006.
- [Girshick, 2015] Ross Girshick. Fast r-cnn. In *ICCV*, pages 1440–1448. IEEE, 2015.
- [Gray, 2006] Robert M Gray. Toeplitz and circulant matrices: A review. *Foundations and Trends in Communication and Information Theory*, 2(3):155–239, 2006.
- [He et al., 2016] Kaiming He, Xiangyu Zhang, Shaoqing Ren, and Jian Sun. Deep residual learning for image recognition. In *CVPR*, pages 770–778. IEEE, 2016.
- [Hu et al., 2010] Zhe Hu, Jia-Bin Huang, and Ming-Hsuan Yang. Single image deblurring with adaptive dictionary learning. In *ICIP*, pages 1169–1172. IEEE, 2010.
- [Hu et al., 2012] Wei Hu, Jianru Xue, and Nanning Zheng. Psf estimation via gradient domain correlation. *IEEE Transactions on Image Processing*, 21(1):386–392, 2012.
- [Jancsary et al., 2012] Jeremy Jancsary, Sebastian Nowozin, Toby Sharp, and Carsten Rother. Regression tree fields—an efficient, non-parametric approach to image labeling problems. In *CVPR*, pages 2376–2383. IEEE, 2012.
- [Kingma and Ba, 2014] Diederik P Kingma and Jimmy Ba. Adam: A method for stochastic optimization. *arXiv preprint arXiv:1412.6980*, 2014.
- [Krishnan and Fergus, 2009] Dilip Krishnan and Rob Fergus. Fast image deconvolution using hyper-laplacian priors. In *NIPS*, pages 1033–1041. MIT Press, 2009.
- [Kundur and Hatzinakos, 1996] Deepa Kundur and Dimitrios Hatzinakos. Blind image deconvolution. *IEEE Signal Processing Magazine*, 13(3):43–64, 1996.
- [Kupyn et al., 2017] Orest Kupyn, Volodymyr Budzan, Mykola Mykhailych, Dmytro Mishkin, and Jiri Matas. Deblurgan: Blind motion deblurring using conditional adversarial networks. *arXiv preprint arXiv:1711.07064*, 2017.
- [Levin et al., 2007] Anat Levin, Rob Fergus, Frédo Durand, and William T Freeman. Image and depth from a conventional camera with a coded aperture. *ACM Transactions on Graphics*, 26(3):70, 2007.
- [Levin et al., 2009] Anat Levin, Yair Weiss, Fredo Durand, and William T Freeman. Understanding and evaluating blind deconvolution algorithms. In *CVPR*, pages 1964–1971. IEEE, 2009.
- [Lin et al., 2014] Tsung-Yi Lin, Michael Maire, Serge Belongie, James Hays, Pietro Perona, Deva Ramanan, Piotr Dollár, and C Lawrence Zitnick. Microsoft coco: Common objects in context. In *ECCV*, pages 740–755. Springer, 2014.
- [Martin et al., 2001] David Martin, Charless Fowlkes, Doron Tal, and Jitendra Malik. A database of human segmented natural images and its application to evaluating segmentation algorithms and measuring ecological statistics. In *ICCV*, volume 2, pages 416–423. IEEE, 2001.
- [Nah et al., 2017] Seungjun Nah, Tae Hyun Kim, and Kyoung Mu Lee. Deep multi-scale convolutional neural network for dynamic scene deblurring. In *CVPR*, pages 3883–3891. IEEE, 2017.
- [Perrone and Favaro, 2014] Daniele Perrone and Paolo Favaro. Total variation blind deconvolution: The devil is in the details. In *CVPR*, pages 2909–2916. IEEE, 2014.
- [Ren et al., 2015] Dongwei Ren, Hongzhi Zhang, David Zhang, and Wangmeng Zuo. Fast total-variation based image restoration based on derivative augmented lagrangian method. *Neurocomputing*, 2015.
- [Ren et al., 2016] Wenqi Ren, Xiaochun Cao, Jinshan Pan, Xiaojie Guo, Wangmeng Zuo, and Ming-Hsuan Yang. Image deblurring via enhanced low-rank prior. *IEEE Transactions on Image Processing*, 25(7):3426–3437, 2016.
- [Ren et al., 2018] Dongwei Ren, Wangmeng Zuo, David Zhang, Jun Xu, and Lei Zhang. Partial deconvolution with inaccurate blur kernel. *IEEE Transactions on Image Processing*, 27(1):511 – 524, 2018.
- [Schmidt and Roth, 2014] Uwe Schmidt and Stefan Roth. Shrinkage fields for effective image restoration. In *CVPR*, pages 2774–2781. IEEE, 2014.
- [Schmidt et al., 2013] Uwe Schmidt, Carsten Rother, Sebastian Nowozin, Jeremy Jancsary, and Stefan Roth. Discriminative non-blind deblurring. In *CVPR*, pages 604–611. IEEE, 2013.
- [Wang et al., 2004] Zhou Wang, Alan C Bovik, Hamid R Sheikh, and Eero P Simoncelli. Image quality assessment: from error visibility to structural similarity. *IEEE Transactions on Image Processing*, 13(4):600–612, 2004.

- [Wang *et al.*, 2008] Yilun Wang, Junfeng Yang, Wotao Yin, and Yin Zhang. A new alternating minimization algorithm for total variation image reconstruction. *SIAM Journal on Imaging Sciences*, 1(3):248–272, 2008.
- [Xu *et al.*, 2014a] Li Xu, Jimmy SJ Ren, Ce Liu, and Jiaya Jia. Deep convolutional neural network for image deconvolution. In *NIPS*, pages 1790–1798. MIT Press, 2014.
- [Xu *et al.*, 2014b] Li Xu, Xin Tao, and Jiaya Jia. Inverse kernels for fast spatial deconvolution. In *ECCV*, pages 33–48. Springer, 2014.
- [Yang *et al.*, 2017] Chao Yang, Xin Lu, Zhe Lin, Eli Shechtman, Oliver Wang, and Hao Li. High-resolution image inpainting using multi-scale neural patch synthesis. In *CVPR*, volume 1, page 3. IEEE, 2017.
- [Zhang *et al.*, 2010] Xiaoqun Zhang, Martin Burger, Xavier Bresson, and Stanley Osher. Bregmanized nonlocal regularization for deconvolution and sparse reconstruction. *SIAM Journal on Imaging Sciences*, 3(3):253–276, 2010.
- [Zhang *et al.*, 2017] Kai Zhang, Wangmeng Zuo, Shuhang Gu, and Lei Zhang. Learning deep cnn denoiser prior for image restoration. In *CVPR*, pages 3929–3938. IEEE, 2017.